Submitted to *Journal of Geophysical Research* (Space Physics): June 16, 1999.

Magnetic Field Strength Distribution in Interplanetary Turbulence

T. Hartlep[1], W. H. Matthaeus, N. S. Padhye and C. W. Smith

Bartol Research Institute, University of Delaware, Newark, DE 19716

Abstract. The distribution of magnetic field magnitudes is derived for the special case of a constant mean field and uncorrelated components having Gaussian distributions. Of the three cases considered– isotropic, transverse, and axisymmetric, the latter most closely resembles a lognormal distribution, when the parallel variance is less than the perpendicular variance. Thus, a normally distributed, non-intermittent vector field can produce a magnitude distribution that closely resembles a functional form often associated with models of intermittency. This result is illustrated by comparison with a magnetic field magnitude distribution computed from the 1 AU Omni dataset. The parameters of the Gaussian component magnitude distribution can be chosen to compare with the data which is also well fit as a lognormal type. We conclude that the magnitude distribution may not be a sensitive indicator of intermittency, and that further examination of the sensitivity of such indicators is warranted.

1. Introduction

The magnetic field magnitudes in the heliosphere has been shown to be approximately described by a lognormal distribution [*Burlaga and King*, 1979; *Slavin and Smith*, 1983; *Burlaga and Ness*, 1998], but there exist no theoretical model we are aware of which predicts such a distribution of the field strength. Often the lognormal distribution is employed in simple models for intermittency in turbulence [see, e.g., *Monin and Yaglom*, 1975]. However, there seems to be no compelling reason to assert that the lognormal functional form is fundamental in the interplanetary context, nor is it clear that there is a connection between the intermittency of the vector fluctuations and the approximate lognormality of the magnitude distribution, although both these features are observed [*Feynman and Ruzmaikin*, 1994]. Indeed, the magnitude of the field comprises both the local mean, which is intrinsically related to features of the large scale coronal expansion, and fluctuations, which may be related to local phenomena, including turbulence. Thus it is not entirely clear whether statistical properties of the mean field are controlled by *in situ* processes, such as an intermittent turbulent cascade. Nevertheless there seems to be a presumed connection between lognormality and intermittency of a turbulent vector field or its derivatives. For these reasons we are motivated to examine in the present paper the degree to which Gaussian fluctuations, which are purely "non-intermittent," might be distinguished from fluctuations that give rise to lognormal distributions of the field magnitude. As a reminder, the probablility distribution function (PDF) of a lognormally distributed process B is defined as:

$$f_{logn}(B) = \frac{1}{\sqrt{2\pi} wB} \exp\Big\{ - \frac{(\ln \frac{B}{B_c})^2}{2w^2} \Big\}. \qquad (1)$$

Note that the quantity $\ln B$ is normally distributed. Defining the ensemble average by $\langle \ldots \rangle$, the parameters B_c and w defining the distribution f_{logn} are determined as $\ln B_c = \langle \ln B \rangle$ and $w^2 = \langle (\ln B - \ln B_c)^2 \rangle$.

[1] Now at Universität Bayreuth, Bayreuth, Germany

2. Gaussian Fluctuations With Constant Mean

Let us denote the magnetic field in so-called mean field coordinates (MFC), which are cartesian coordinates with unit vectors $\mathbf{e}_{\perp 1}$, $\mathbf{e}_{\perp 2}$ and $\mathbf{e}_{||}$ such that the instantaneous ensemble mean field $\mathbf{B}_0 = \langle \mathbf{B} \rangle$ always points along positive $\mathbf{e}_{||}$ direction. In this section we assume that the absolute value, denoted by B_0, of the ensemble mean field is a constant for all time. The magnetic field vector $\mathbf{B}$ in MFC may therefore be decomposed into a constant mean plus fluctuations $\mathbf{b}$:

$$\mathbf{B} = B_0 \mathbf{e}_{||} + \mathbf{b}. \qquad (2)$$

Let us assume, as mentioned earlier, that the MFC components of the fluctuations can be approximated by Gaussian distributions [*Whang*, 1977] with variances $\sigma^2_{\perp 1}$, $\sigma^2_{\perp 2}$ and $\sigma^2_{||}$, respectively. In that case the probability distribution functions for the components of the fluctuations are:

$$f_i(b_i) = \frac{1}{\sqrt{2\pi}\sigma_i} \exp\{-\frac{b_i^2}{2\sigma_i^2}\}, \quad i = \perp 1, \perp 2, ||. \qquad (3)$$

For simplicity we assume that these components are uncorrelated and therefore the magnetic field vector's probability distribution function is just the product of the probability distributions of its components, i.e:

$$\begin{aligned} f_{\mathbf{B}}(\mathbf{B}) &= f_{\mathbf{B}}(B_{\perp 1}, B_{\perp 2}, B_{||}) \qquad (4)\\ &= f_{\perp 1}(B_{\perp 1}) f_{\perp 2}(B_{\perp 2}) f_{||}(B_{||} - B_0). \end{aligned}$$

The probability for observing simultaneously the first perpendicular component of the magnetic field between $B_{\perp 1}$ and $B_{\perp 1} + dB_{\perp 1}$, the second perpendicular component between $B_{\perp 2}$ and $B_{\perp 2} + dB_{\perp 2}$ and the field's parallel component between $B_{||}$ and $B_{||} + dB_{||}$ is therefore given by:

$$f_{\mathbf{B}}(B_{\perp 1}, B_{\perp 2}, B_{||}) dB_{\perp 1} dB_{\perp 2} dB_{||},$$

which may be written in spherical coordinates as:

$$f_{\mathbf{B}}(B\cos\phi\sin\theta, B\sin\phi\sin\theta, B\cos\theta) B^2 d(\cos\theta) d\phi dB,$$

where $B \equiv |\mathbf{B}|$ is the magnitude of the magnetic field. If we carry out the integration over θ and ϕ we are left with the probability for the magnitude to lie between B and $B + dB$, i.e. the Gaussian component magnitude distribution (GCMD) is therefore:

$$f(B; B_0, \sigma^2_{\perp 1}, \sigma^2_{\perp 2}, \sigma^2_{||}) = \int_{-1}^{1} d(\cos\theta) \int_0^{2\pi} d\phi B^2 f_{\mathbf{B}} \qquad (5)$$

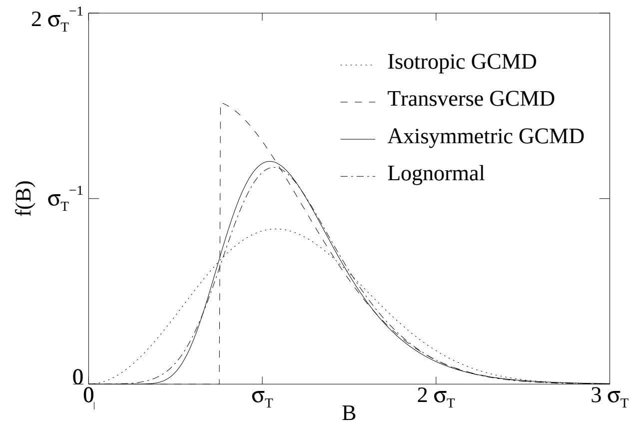

Figure 1. Typical shapes of isotropic, transverse and axisymmetric Gaussian component magnitude distributions (GCMDs), each with the same mean field B_0 and the total variance $\sigma_T^2 := \sigma^2_{\perp 1} + \sigma^2_{\perp 2} + \sigma^2_{||}$.

where

$$f_{\mathbf{B}} = (B\cos\phi\sin\theta,\ B\sin\phi\sin\theta,\ B\cos\theta). \qquad (6)$$

In the following we examine three possible symmetries of the fluctuations.

2.1. Isotropic Fluctuations

At first let us consider the case of fully isotropic fluctuations, i.e. the variances $\sigma^2_{\perp 1}$, $\sigma^2_{\perp 2}$ and $\sigma^2_{||}$ have the same value, which may be called σ^2. For convenience, we define the total variance $\sigma_T^2 = \sigma^2_{\perp 1} + \sigma^2_{\perp 2} + \sigma^2_{||}$. The isotropic geometry greatly simplifies Eq. (6) and the double integral can be done easily. The isotropic GCMD is then given by:

$$f_{iso}(B; B_0, \sigma^2) = \sqrt{\frac{2}{\pi}} \frac{B}{B_0 \sigma} \exp\{-\frac{B^2 + B_0^2}{2\sigma^2}\} \sinh\{\frac{B B_0}{\sigma^2}\}. \qquad (7)$$

For the sake of reference, we compute a lognormal distribution to have the same first and second moments, $\langle B \rangle$ and $\langle B^2 \rangle$, as the axisymmetric geometry example described below. The resulting lognormal function is shown in Figure 1 and represented as a dot-dashed curve.

The dotted curve in Figure 1 shows the functional form of Eq. 7. For all three Gaussian component predictions shown in Figure 1, we express the functions in terms of σ_T, the square root of the total variance.

Both B and B_0 are expressed in units of σ_T and $f(B)$ is in units of $1/\sigma_T$. The lognormal function is computed as above and expressed in terms of these same units. We use $B_0 = 0.76\sigma_T$ for all examples shown in Figure 1. We observe that the resulting PDF for the isotropic geometry is not a particularly good match for the lognormal distribution represented by the dot-dash curve. The match is not too bad for $B > 1.5\sigma_T$, but the peak region is relatively low and broad and the low-B interval exceeds the lognormal form. Overall, the functional form does not resemble the lognormal. We will see below that a high degree of anisotropy favors comparison with the lognormal form.

2.2. Transverse Fluctuations

The next case is that of purely transverse turbulence that is axisymmetric, i.e., isotropic in the plane perpendicular to the mean magnetic field. This means that there are no fluctuations parallel to the mean field, i.e. $\sigma_{||}^2 = 0$, and the variances of the fluctuations perpendicular to $\mathbf{B}_0$ are equal, i.e. $\sigma_\perp^2 := \sigma_{\perp 1}^2 = \sigma_{\perp 2}^2$. Although this is a slight exaggeration due to the $\sigma_{||}^2 = 0$ assumption, it approximates the familiar example of *Belcher and Davis* [1971] who observed that fluctuations within and behind high-speed streams were largely transverse to the mean magnetic field. A number of other studies have confirmed this anisotropy, for example, at 1AU using ISEE-3 data [*Matthaeus et al.*,1986], and over varying heliocentric distances in the Voyager datasets [*Klein et al.*, 1991]. In each case there was observed a distinct tendency for the variance anisotropy to be relatively greater in shorter intervals (several hours or less) with a greater tendency for isotropy seen in datasets of a day or more duration. Ulysses observations [*Phillips et al.*, 1995; *Horbury et al.*, 1995] have confirmed this aspect of the high latitude IMF as a general attribute of high-speed winds, except for fluctuations at even lower frequencies which are transverse to the radial direction [*Smith et al.*, 1995]. *Leamon et al.* [1998] demonstrated that fluctuations within magnetic clouds are even more nearly transverse to the local mean field than in typical high-speed streams at 1 AU. Purely transverse variances are also a property of simple but familiar "slab models" of parallel propagating Alfvén waves, often invoked as a traditional leading order description of solar wind fluctuations [*Jokipii*, 1966].

In the present model, for purely transverse fluctuations, $\sigma_{||}^2 = 0$, and the distribution function of the parallel component $b_{||}$ degenerates to a δ-function:

$$f_{||}(b_{||}) = \delta(b_{||}) = \delta(B_{||} - B_0) = \delta(B\cos\theta - B_0). \quad (8)$$

Using $\delta(B\cos\theta - B_0) = B^{-1}\delta(\cos\theta - B_0/B)$ we can write the transverse Gaussian component magnitude distribution (transverse GCMD) as:

$$f_{trans}(B; B_0, \sigma_\perp^2) = \begin{cases} 0 & \text{for } B < B_0 \\ \frac{B}{\sigma_\perp^2}\exp\left\{\frac{B_0^2 - B^2}{2\sigma_\perp^2}\right\} & \text{for } B > B_0 \end{cases}. \quad (9)$$

Note that $f_{trans}(B; B_0, \sigma_\perp^2) = 0$ when $B < B_0$ because any perpendicular fluctuations necessarily increase the magnitude of the field beyond B_0. Only fluctuations in the parallel component can reduce the magnitude, but these are absent in the present case.

The dashed curve in Figure 1 shows the functional form of Eq. 9 for the same mean B_0 and total variance used to compute the dotted curve for the isotropic geometry. For $B < B_0$, the agreement is poor as expected due to the extreme approximation that $\sigma_{||}^2 = 0$, but the function quickly assumes a form that is in good agreement with the lognormal once the peak of the lognormal is achieved. In part, this demonstrates the need for anisotropy in obtaining a PDF for the components that produces a good fit to the lognormal form for the magnitude distribution cited by *Burlaga and Ness* [1998].

2.3. Axisymmetric Fluctuations

The last and, as we see later, the most important case is that of axisymmetry, where, as above, the perpendicular variances $\sigma_{\perp 1}^2$ and $\sigma_{\perp 2}^2$ have the same value $\sigma_\perp^2$, but there is a non-zero parallel variance $\sigma_{||}^2$. Equations. (3)–(6) yield for the axisymmetric GCMD, after integration over ϕ the following expression:

$$f_{axis}(B; B_0, \sigma_\perp^2, \sigma_{||}^2) = \quad (10)$$
$$\int_{-1}^{1} d(\cos\theta)\frac{B^2}{\sqrt{2\pi}\sigma_\perp^2\sigma_{||}}\exp\left\{-\,,\,(B, B_0, \sigma_\perp^2, \sigma_{||}^2)\right\},$$

where

$$,\,(B, B_0, \sigma_\perp^2, \sigma_{||}^2) = \quad (11)$$
$$\frac{B^2}{2\sigma_\perp^2} + \frac{B_0^2}{2(\sigma_\perp^2 - \sigma_{||}^2)} + \frac{B^2(\sigma_\perp^2 - \sigma_{||}^2)}{2\sigma_\perp^2\sigma_{||}^2}\left(\cos\theta - \frac{B_0\sigma_\perp^2}{B(\sigma_\perp^2 - \sigma_{||}^2)}\right)^2.$$

After changing the integration variable to

$$\sqrt{\frac{B^2|\sigma_\perp^2 - \sigma_{||}^2|}{2\sigma_\perp^2\sigma_{||}^2}}\left(\cos\theta - \frac{B_0\sigma_\perp^2}{B(\sigma_\perp^2 - \sigma_{||}^2)}\right), \quad (12)$$

we arrive at the result:

$$f_{axis}(B;B_0,\sigma_\perp,\sigma_{||}) = \begin{cases} C_1 B f^{erf} & \text{for } \sigma_\perp > \sigma_{||} \\ C_1 B f^{erfi} & \text{for } \sigma_\perp < \sigma_{||} \end{cases}, \quad (13)$$

where

$$\begin{aligned} f^{erf} &= \exp\left\{-\frac{B^2}{2\sigma_\perp^2}\right\}\left(\mathrm{erf}\{C_2B+C_3\}+\mathrm{erf}\{C_2B-C_3\}\right) \\ f^{erfi} &= \exp\left\{-\frac{B^2}{2\sigma_\perp^2}\right\}\left(\mathrm{erfi}\{C_2B+C_3\}+\mathrm{erfi}\{C_2B-C_3\}\right\} \end{aligned}$$

and

$$\begin{aligned} C_1 &= \frac{1}{2\sigma_\perp\sqrt{|\sigma_\perp^2-\sigma_{||}^2|}}\exp\left\{\frac{B_0^2}{2(\sigma_\perp^2-\sigma_{||}^2)}\right\}, \\ C_2 &= \sqrt{\left|\frac{1}{2\sigma_\perp^2}-\frac{1}{2\sigma_{||}^2}\right|}, \\ C_3 &= \frac{B_0\sigma_\perp}{2\sigma_{||}\sqrt{|\sigma_\perp^2-\sigma_{||}^2|}}. \end{aligned} \quad (14)$$

Here $\mathrm{erf}(x) = 2\pi^{-1/2}\int_0^x \exp\{-x^2\}dx$ is the error function and $\mathrm{erfi}(x) = 2\pi^{-1/2}\int_0^x \exp\{x^2\}dx$ is the imaginary error function.

The solid curve in Figure 1 shows the functional form of Eq. 13 for the same mean B_0 and total variance used in the previous two examples. In addition, we take $\sigma_\perp^2 = 10\times\sigma_{||}^2$ in order to introduce a degree of anisotropy consistent with *Belcher and Davis* [1971] and *Horbury et al.* [1995]. This function now offers a good approximation to the lognormal throughout the entire range of B.

3. Data Analysis

We now apply the above theoretical development to the observed PDF for B. We analyze NSSDC Omnitape data [*King and Papitashvili*, 1994] consisting of 1 hour magnetic field averages over a 30 year span from 1966 through 1995. Four-day subintervals are chosen and those with more than 25% bad or missing points are dropped from the analysis. Subintervals that exhibit strong variations are also dropped since they are likely to represent non-quiescent intervals of the solar wind plasma, such as shocks and current sheet observations. The criterion used to detect such intervals with strong variation is $\sigma_T^2/B_0^2 > 2.0$, where σ_T^2 is the sum of the variances of the three magnetic field components, and B_0 is the mean field magnitude of that interval. The analysis is carried out in the mean field coordinate system [*Belcher and Davis*, 1971], where one axis is along the mean field, while the other two axes are perpendicular to it. Figure 2 shows the resulting PDF of B when computed in the way.

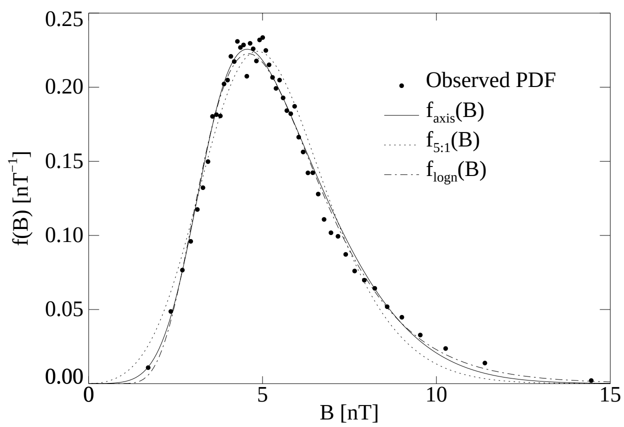

Figure 2. Best fit axisymmetric GCMDs (solid curve - B_0, $\sigma_\perp^2$ and $\sigma_{||}^2$ are free parameters, dotted curve - fixed anisotropy of 5:5:1) and best fit lognormal distribution (dash-dotted curve). The observed distribution of the field magnitude is shown by the dots.

	χ^2	Best-Fit Parameters
$f_{axis}(B)$	0.0041	$\sigma_\perp^2 = 12.20$, $\sigma_{||}^2 = 0.82$, $B_0 = 2.96$
$f_{5:1}(B)$	0.0128	$\sigma_\perp^2 = 5\cdot\sigma_{||}^2$, $\sigma_{||}^2 = 1.98$, $B_0 = 3.10$
$f_{logn}(B)$	0.0035	$w^2 = 0.1334$, $B_c = 5.25$

Table 1. Parameterizations for Figure 2

We perform a best-fit analysis of the distribution using two different probability distribution functions described in the previous section: Lognormal, and Axisymmetric GCMD. In these best-fit analysis of the Lognormal distribution, both parameters, w and B_c (see Eq. (1)) are allowed to vary. For the Axisymmetric GCMD, B_0, $\sigma_\perp$, and $\sigma_{||}$ are allowed to vary. As a third example, we fit an Axisymmetric GCMD that assumes a $5:1$ ratio of $\sigma_\perp^2 : \sigma_{||}^2$, but allow the total variance σ_T^2 and B_0 to vary. These three fits are denoted by $f_{logn}(B)$, $f_{axis}(B)$, and $f_{5:1}(B)$ respectively in table 1. These functions are also shown in Figure 2. All three represent good approximations to both the data and the lognormal form, although the $5:1$ Axisymmetric GCMD function shows some notable departure at both high- and low-B.

The goodness-of-fit for these three cases is measured by χ^2, which is defined as

$$\chi^2 = \frac{\Sigma_i \left(f_1(B_i) - f_2(B_i)\right)^2 \Delta B_i}{\Sigma_i f_1^2(B_i)\, \Delta B_i},$$

where $f_1(B_i)$ is the observed PDF, $f_2(B_i)$ is one of the theoretical functions mentioned above, and ΔB_i is the bin-width of the observed data at B_i. In table 1 we list the χ^2 values and the corresponding best-fit parameters for the three cases. Note that the χ^2 values are virtually identical for the axisymmetric GCMD and the lognormal distribution.

4. Discussion

We have shown that a vector field with a fixed mean and normally distributed (Gaussian) components gives rise to a distribution of vector magnitudes that under suitable conditions is quite similar in form to a lognormal distribution. In particular, the correspondence is good when the Gaussian component magnitude distribution is axisymmetric about the mean field but admits a high degree of variance anisotropy, with parallel variance less than perpendicular variance. Lognormal distributions are encountered in a wide variety of circumstances in space physics [*Burlaga and Ness*, 1998; *Feynman and Ruzmaikin*, 1994; *Angelopoulos et al.*, 1999] and are often taken as indicators of scale invariant or statistically intermittent processes. The present calculation shows that this correspondence must be interpreted with some care, since a very similar distribution can be recovered in an entirely different way for the magnitude of a vector field. A Gaussian distribution for the components need not imply scale invariance (although there is no contradiction if it does) and in any case it is, by definition, non-intermittent. In deriving this result, we assumed independence of the component distributions, an exact result in planes of symmetry, but one that requires further scrutiny for the general case.

We illustrated this idea in the context of solar wind fluctuations observed at 1 AU. Although the theory described here offers a good fit to the observed distribution of B, it raises some questions in connection with existing knowledge of solar wind fluctuations. For instance, the best-fit version of the theory requires an unusually high degree of fluctuation anisotropy which may not be supported by the data. In addition, the theory assumes a constant B_0 value when the above analysis of the data produces a distribution of B_0 values (not shown) that itself crudely resembles a lognormal distribution. This raises the further question as to whether the statistical properties of the magnitude of the total magnetic field are controlled by variability of the mean field (as might be defined, for example, by a suitable time average) or variability of the fluctuations. The implications may differ considerably, as the former is likely controlled by coronal conditions, whereas the latter may be influenced greatly by active *in situ* processes, including turbulence which may generate intermittency and non-gaussian statistical effects.

There is a considerable body of evidence that solar wind fluctuations display statistical properties that are non-Gaussian and intermittent [*Burlaga and Ness*, 1998; *Feynman and Ruzmaikin*, 1994; *Tu et al.*, 1996; *Horbury et al.*, 1996]. Less well understood is the origin of these properties, whether they might be of local or coronal origin, or whether they are of a dynamical or kinematic character. There also remain questions as to whether distinctive non-gaussian distributions are associated principally with small scale dissipative intermittency, or with large scale flows or time dependent features of the solar wind. The prospect for clear answers to these questions is complicated further by relatively unexplored issues pertaining to the sensitivity of statistical distributions and high order moments to averaging techniques, data selection criteria and finite sample effects [see e.g., *Matthaeus et al.*, 1986; *Feynman and Ruzmaikin*, 1994]. We intend to explore these issues in greater detail in the future, concluding at present only that the appearance of approximately lognormal distributions of vector magnitudes may not be a sensitive indicator of underlying non-gaussian statistics.

Acknowledgments. This work was supported by NASA grants NAG5-6570, NAG5-3026 and NAG5-8134.

References

Angelopoulos, V., T. Mukai and S. Kokubun, Evidence for intermittency in earth's plasma sheet and implications for self organized criticality, *Phys. Plasmas*, submitted, 1999.

Belcher, J. W., and L. Davis Jr., Large-amplitude Alfvén waves in the interplanetary medium, 2, *J. Geophys. Res.*, *76*, 3534–3563, 1971.

Burlaga, L. F., and J. H. King, Intense interplanetary magnetic fields observed by geocentric spacecraft during 1963-1975, *J. Geophys. Res.*, *84*, 6633, 1979.

Burlaga, L. F., and N. F. Ness, Magnetic field strength distributions and spectra in the heliosphere and their significance for cosmic ray modulation: Voyager 1, 1980–1994, *J. Geophys. Res.*, *103*, 29,719–29,732, 1998.

Feynman, J., and A. Ruzmaikin, Distributions of the interplanetary magnetic field revisited, *J. Geophys. Res.*, *99*, 17,645–17,651, 1994.

Horbury, T. S., A. Balogh, R. J. Forsyth, and E. J. Smith, Anisotropy of inertial range turbulence in the polar heliosphere, *Geophys. Res. Lett.*, *22*, 3405–3408, 1995.

Horbury, T. S., A. Balogh, R. J. Forsyth, and E. J. Smith, Magnetic field signatures of unevolved turbulence in polar flows, *J. Geophys. Res.*, *101*, 405–413, 1996.

King, J. H., and N. E. Papitashvili, Interplanetary Medium Data Book — Supplement 5, 1988–1993, (Rep. NSSDC/ WDC–A–R&S 94–08, NASA, Greenbelt, Md) 1994.

Klein, L. W., and D. A. Roberts and M. L. Goldstein, Anisotropy and Minimum Variance Directions of Solar Wind Fluctuations in the Outer Heliosphere, *J. Geophys. Res.*, *96*, 3779–3788, 1991.

Leamon, R. J., C. W. Smith and N. F. Ness, Characteristics of magnetic fluctuations within coronal mass ejections: The January 1997 event, *Geophys. Res. Lett.*, *25*, 2505–2509, 1998.

Matthaeus, W. H., M. L. Goldstein and J. H. King, An interplanetary magnetic field ensemble at 1 AU, *J. Geophys. Res.*, *91*, 59–69, 1986.

Monin, A.S., and A. M. Yaglom, *Statistical Fluid Mechanics*, MIT Pres, Cambridge, MA, 1975.

Phillips, J. L., et al., Ulysses solar wind plasma observations from pole to pole, *Geophys. Res. Lett.*, *22*, 3301–3304, 1995.

Slavin, J. A., and E. J. Smith, Solar cycle variations in the interplanetary magnetic field, in Solar Wind Five, *NASA Conf. Pub.*, *2280*, 323–331, 1983.

Smith, E. J., A. Balogh, M. Neugebauer, and D. McComas, Ulysses observations of Alfvén waves in the southern and northern solar hemispheres, *Geophys. Res. Lett.*, *22*, 3381–3384, 1995.

Tu, C.Y., et al., An extended structure-function model and its application to the analysis of solar wind intermittency properties, *Ann. Geophysicae*, *14*, 270–285, 1996.

Whang, Y. C., Probability distribution function of mesoscale magnetic fluctuations during quiet conditions, *Solar Physics*, *53*, 507–517, 1977.

T. Hartlep, W. H. Matthaeus, N. S. Padhye, and C. W. Smith, Bartol Research Institute, University of Delaware, Newark, DE 19716.
(e-mail: [hartlep, yswhm, nikhil, chuck]@bartol.udel.edu)

This preprint was prepared with AGU's LaTeX macros v4. File hartlep formatted June 15, 1999.

With the extension package 'AGU++', version 1.2 from 1995/01/12